NACA TN 2694

NATIONAL ADVISORY COMMITTEE FOR AERONAUTICS

TECHNICAL NOTE 2694

A METHOD FOR STABILIZING SHOCK WAVES IN CHANNEL FLOW BY MEANS OF A SURGE CHAMBER

By Stanford E. Neice

Cornell University

PROPERTY FAIRCHILD
ENGINEERING LIBRARY

JUN 22 1953

Washington
June 1953

NATIONAL ADVISORY COMMITTEE FOR AERONAUTICS

TECHNICAL NOTE 2694

A METHOD FOR STABILIZING SHOCK WAVES IN CHANNEL FLOW BY MEANS OF A SURGE CHAMBER[1]

By Stanford E. Neice[2]

SUMMARY

In order to stabilize normal shock waves in channel flow against the effect of disturbances originating downstream, a method based on mass removal from the channel by means of a surge chamber was developed and experimentally tested in an intermittent blowdown-type wind tunnel at Cornell University. A theoretical analysis of the flow in a channel shape similar to that used in a typical double-throat supersonic wind tunnel indicated that the mass-removal technique was effective in damping the motion of the normal shock caused by a strong compression pulse originating downstream. The results of experimental tests were in quantitative agreement with the theoretical analysis. Further experiments indicated that the mass-removal technique was effective in damping the oscillatory motion of the normal shock caused by continuous small, random, downstream disturbances.

INTRODUCTION

An important factor in the design and operation of supersonic wind tunnels is their large power consumption. A large part of this loss results from the fact that supersonic channel flow can be converted into subsonic flow only through a normal shock wave (see ref. 1). A successful method for reducing this power loss is to lower the Mach number at which the shock occurs. This method has led to the use of the "double-throat" type of supersonic wind tunnel.

For the most efficient operation of the double-throat wind tunnel, the normal shock is placed in a position just downstream of the second minimum section. However, disturbances originating downstream in the diffusor and exhaust system will interact with the normal shock and cause

[1]The body of this report is a thesis which was submitted in February 1950 in a partial fulfillment of the requirements for the degree of Master of Aeronautical Engineering in the Graduate School of Aeronautical Engineering, Cornell University, Ithaca, New York.

[2]Now at the Ames Aeronautical Laboratory, Moffett Field, Calif.

it to be displaced from its original position. If these disturbances are strong enough, they can cause the shock to be permanently displaced to a position upstream of the test section. Subsonic flow will then exist in the test section and the wind tunnel is said to be "unstarted." In order to avoid this highly undesirable condition, it is often necessary to place the normal shock quite far downstream of the second minimum section. Operation with the shock far downstream of the second throat results in an increased power loss and defeats partially the purpose of the second minimum section.

The power consumption of the double-throat wind tunnel could be reduced if there were a suitable method for stabilizing the normal shock against the effect of these disturbances, thus permitting the shock to be placed closer to the second minimum section. It is the purpose of this paper to show how the use of a surge chamber, connected to the channel immediately upstream of the operating position of the normal shock, can produce the desired stability.

The author is grateful to Professor Arthur R. Kantrowitz for his suggestion of the topic, advice throughout the investigation, and for the information contained in Appendixes A and B.

SYMBOLS

A	area of transverse slit
a	speed of sound
c_p	specific heat at constant pressure
c_v	specific heat at constant volume
M	Mach number
m	mass flow
P	characteristic quantity, $\frac{2c_v}{R} a + u$
p	pressure
Q	characteristic quantity, $\frac{2c_v}{R} a - u$
R	gas constant
S	area of channel
T	temperature
t	time

U	velocity of shock wave
u	velocity of fluid
x	station along channel
γ	ratio of specific heats
ρ	density
η	entropy

Subscripts

a	conditions behind steady-flow normal shock
b	conditions behind leading edge of pulse
c	conditions at rear of pulse
s	conditions relative to moving shock wave
o	standard conditions
1,2,3,4,5	conditions in various sectors of the characteristic diagram

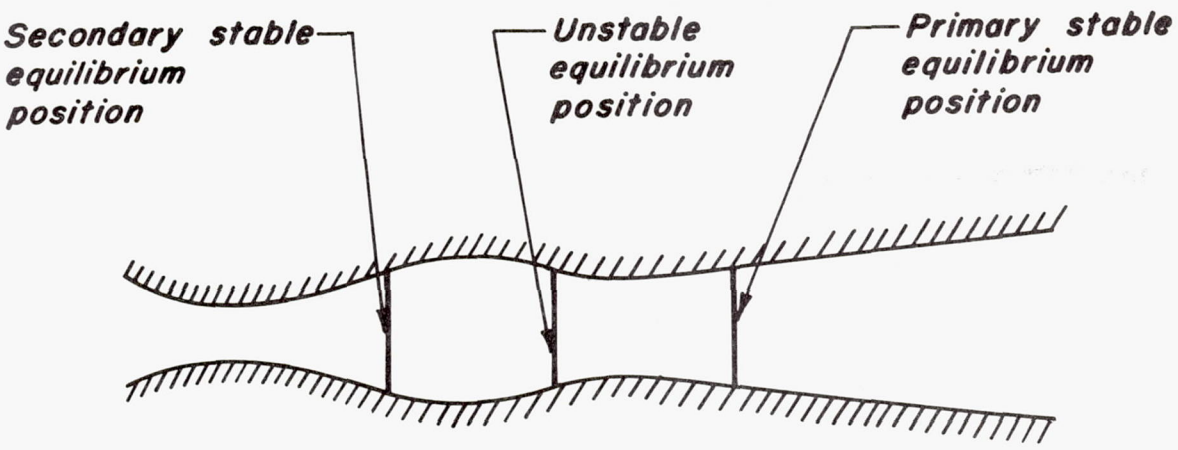
Superscript

-	average values

THEORETICAL CONSIDERATIONS

Stability of Normal Shock Waves in Channel Flow

In the normal operating condition of a conventional double-throat supersonic wind tunnel, the shock wave converting the supersonic flow to subsonic flow will occur downstream of the second minimum section as shown in sketch (a). The normal shock wave in this case is in its primary stable equilibrium position which means that it will return to this position after undergoing small displacements.



Sketch (a)

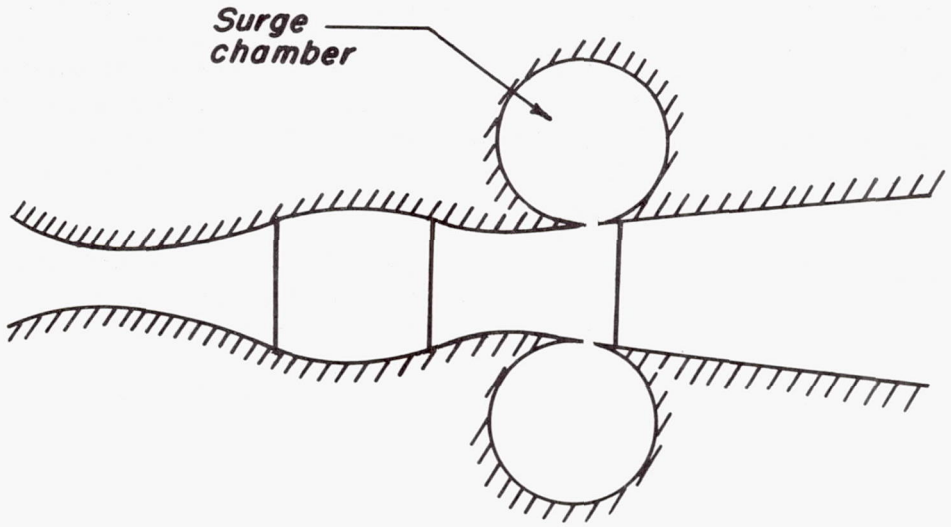
There are two other equilibrium positions, also shown in sketch (a), which occur at points in the channel where the channel area is the same as the area at the primary stable equilibrium position. At the indicated position in the converging part of the channel, the normal shock is in a condition of unstable equilibrium. Consequently, if the shock were to exist in this position, then any displacement, however small, would cause the shock to assume either stable position, depending upon the direction of the displacement.

Displacement of the normal shock from the primary equilibrium position can be caused by disturbances originating downstream. These disturbances propagate upstream through the subsonic flow in the diffusor section and interact with the main shock. The resultant shock is then set in motion and will undergo a displacement proportional to the strength of the disturbance. As pointed out in reference 1, a compression disturbance will cause the shock to be displaced upstream in the direction of the unstable equilibrium position. If the compression disturbance is strong enough to cause a displacement of the shock upstream of the unstable equilibrium position, then, as has been pointed out, the shock will assume the secondary stable equilibrium position shown in sketch (a). Subsonic flow will then exist in the test section, and the tunnel will be unstarted.

Operation of the Surge Chamber

In the method presented herein, the shock position is stabilized by the appropriate use of a surge chamber, which, in effect, creates a counterdisturbance which neutralizes the action of a compression disturbance coming from downstream.

The surge chamber is connected to the channel (see sketch (b)) by transverse slits at a point just upstream of the primary equilibrium position. In the normal running condition, the surge chamber is at the same pressure as that existing in the channel at the position of the slits. The normal shock, set in motion by interaction with a compression disturbance, crosses the slits, thus raising the pressure in the channel, and causes air to flow out of the channel into the surge chamber.



Sketch (b)

The removal of mass in this manner, in effect, produces an expansion which propagates throughout the channel. Part of this expansion interacts with the upstream-moving shock wave and dissipates some of the energy supplied by the initial compression disturbance. By varying the opening of the transverse slits, a sufficiently high rate of mass removal may be obtained to bring the shock wave to rest before it passes the unstable equilibrium position. A normal shock brought to rest in this manner will then return to its primary stable equilibrium position downstream of the second minimum section.

By the application of the method of characteristics for nonsteady one-dimensional flow, it is possible to trace the interaction of the normal shock and compression pulse on a time-displacement diagram and to determine the effect of mass removal to the surge chamber. In order to analyze this problem, however, it was necessary to develop an extension to the existing method of characteristics which includes the effects of mass removal from a point in the channel.

The Method of Characteristics Including the Effects of Mass Removal at a Point in the Channel

The method of characteristics for isentropic, inviscid, nonsteady, one-dimensional flow in a channel of constant cross section was first introduced in 1859 by Riemann (ref. 2). In reference 3, the work of Riemann was extended to include variations in entropy and channel area, while in reference 4 the effects of heat transfer were considered in some detail. The general procedure followed in those papers, and exploited in the present analysis, was to define certain characteristic quantities from considerations of the one-dimensional equations of motion and continuity. These characteristic quantities, designated as P and Q,[3] are associated with the two families of characteristics in the flow field.

In the present analysis the equations of continuity and motion are modified to include mass removal from the channel, and the effect of mass removal on the characteristic quantities, P and Q, is determined.

The equation of continuity for one-dimensional flow is

$$S \frac{\partial \rho}{\partial t} + \frac{\partial}{\partial x} (\rho u S) = 0 \tag{1}$$

If, however, mass is removed from the channel through openings in the walls, the continuity equation takes the following form:

$$S \frac{\partial \rho}{\partial t} + \frac{\partial}{\partial x} (\rho u S) + \frac{\partial m}{\partial x} = 0 \tag{2}$$

In the present analysis it is assumed that the mass is removed from the channel at a constant rate $\left(\frac{\partial m}{\partial t} = 0\right)$. Consequently, the equation of motion for one-dimensional flow remains unchanged as

$$\frac{\partial u}{\partial t} + u \frac{\partial u}{\partial x} + \frac{1}{\rho} \frac{\partial p}{\partial x} = 0 \tag{3}$$

---

[3]These quantities, as used in references 3 and 4 as well as the present analysis, differ only by a factor of 2 from the Riemann invariants as given in reference 5.

With the aid of the first law of thermodynamics, the equation for the entropy of a perfect gas can be written in the following differential forms:

$$\left.\begin{aligned} \frac{d\eta}{R} &= \frac{2c_v}{R}\, d(\log_e a) - d(\log_e \rho) \\ \frac{d\eta}{R} &= \frac{2c_p}{R}\, d(\log_e a) - d(\log_e p) \end{aligned}\right\} \tag{4}$$

By the use of equations (4) and the equation of state for a perfect gas in the form $p/\rho = RT$, equations (2) and (3) can be brought into the following forms, respectively:

$$\left.\begin{aligned} &\frac{2c_v}{R}\frac{\partial a}{\partial t} + \frac{2c_v}{R}\, u\frac{\partial a}{\partial x} + a\frac{\partial u}{\partial x} + ua\frac{\partial(\log_e S)}{\partial x} - \\ &\frac{a}{R}\left(\frac{\partial \eta}{\partial t} + u\frac{\partial \eta}{\partial x}\right) + \frac{a}{\rho S}\frac{\partial m}{\partial x} = 0 \end{aligned}\right\} \tag{5}$$

$$\frac{\partial u}{\partial t} + u\frac{\partial u}{\partial x} + \frac{2c_v}{R}\, a\frac{\partial a}{\partial x} - \frac{a^2}{\gamma R}\frac{\partial \eta}{\partial x} = 0 \tag{6}$$

By adding and subtracting equation (6) from equation (5), the following relations are obtained:

$$\left.\begin{aligned} &\frac{\partial}{\partial t}\left(\frac{2c_v}{R}\, a + u\right) + (u + a)\frac{\partial}{\partial x}\left(\frac{2c_v}{R}\, a + u\right) + ua\frac{\partial(\log_e S)}{\partial x} - \\ &\frac{a^2}{\gamma R}\frac{\partial \eta}{\partial x} - \frac{a}{R}\frac{D\eta}{Dt} + \frac{a}{\rho S}\frac{\partial m}{\partial x} = 0 \\ &\frac{\partial}{\partial t}\left(\frac{2c_v}{R}\, a - u\right) + (u - a)\frac{\partial}{\partial x}\left(\frac{2c_v}{R}\, a - u\right) + ua\frac{\partial(\log_e S)}{\partial x} + \\ &\frac{a^2}{\gamma R}\frac{\partial \eta}{\partial x} - \frac{a}{R}\frac{D\eta}{Dt} + \frac{a}{\rho S}\frac{\partial m}{\partial x} = 0 \end{aligned}\right\} \tag{7}$$

where the notation

$$\frac{D}{Dt} = \frac{\partial}{\partial t} + u \frac{\partial}{\partial x} \tag{8}$$

defines an observed rate of change while moving with the fluid particles at a velocity u.

The characteristic quantities, P and Q, are defined as

$$\left.\begin{aligned} P &\equiv \frac{2c_v}{R} a + u \\ Q &\equiv \frac{2c_v}{R} a - u \end{aligned}\right\} \tag{9}$$

and the observed rate of change while moving along a characteristic line in the fluid is defined symbolically as

$$\frac{\delta}{\delta t} = \frac{\partial}{\partial t} + (u \pm a) \frac{\partial}{\partial x} \tag{10}$$

where thc plus (+) or minus (-) signs are associated with P and Q families of characteristics, respectively.

From the definitions of equations (9) and (10), equation (7) can be written as

$$\left.\begin{aligned} \frac{\delta P}{\delta t} &= -ua \frac{\partial(\log_e S)}{\partial x} + \frac{a^2}{\gamma R} \frac{\partial \eta}{\partial x} + \frac{a}{R} \frac{D\eta}{Dt} - \frac{a}{\rho S} \frac{\partial m}{\partial x} \\ \frac{\delta Q}{\delta t} &= -ua \frac{\partial(\log_e S)}{\partial x} - \frac{a^2}{\gamma R} \frac{\partial \eta}{\partial x} + \frac{a}{R} \frac{D\eta}{Dt} - \frac{a}{\rho S} \frac{\partial m}{\partial x} \end{aligned}\right\} \tag{11}$$

which expresses the rate of change of the characteristic quantities along their respective paths.

From equation (10), the following can be deduced:

Along a P characteristic

$$\left.\frac{\delta\eta}{\delta t}\right|_P = \frac{\partial\eta}{\partial t} + (u + a)\frac{\partial\eta}{\partial x} = \frac{D\eta}{Dt} + a\frac{\partial\eta}{\partial x}$$

Along a Q characteristic

$$\left.\frac{\delta\eta}{\delta t}\right|_Q = \frac{\partial\eta}{\partial t} + (u - a)\frac{\partial\eta}{\partial x} = \frac{D\eta}{Dt} - a\frac{\partial\eta}{\partial x}$$

(12)

The channel area of a wind tunnel will depend only on the station along the channel. Consequently, the rate of change of this quantity along P and Q characteristics, with the aid of equation (10), is

$$\left.\frac{\delta(\log_e S)}{\delta t}\right|_P = (u + a)\frac{\partial(\log_e S)}{\partial x}$$

$$\left.\frac{\delta(\log_e S)}{\delta t}\right|_Q = (u - a)\frac{\partial(\log_e S)}{\partial x}$$

(13)

Since the removal of mass from the channel has been assumed to take place at a constant rate, the change in mass flow is, therefore, a function only of the distance along the channel. From equation (10) the rate of change of this quantity along the characteristic lines can be expressed as

$$\left.\frac{\delta m}{\delta t}\right|_P = (u + a)\frac{\partial m}{\partial x}$$

$$\left.\frac{\delta m}{\delta t}\right|_Q = (u - a)\frac{\partial m}{\partial x}$$

(14)

With the aid of equations (12), (13), and (14), and noting that the particle entropy change $D\eta/Dt$ will be zero in the absence of heat transfer and shock waves, the variations in the characteristic quantities will then be

$$\left.\begin{aligned} \delta P &= -\frac{ua}{u+a}\,\delta(\log_e S) + \frac{a}{\gamma R}\,\delta\eta - \frac{a}{\rho S(u+a)}\,\delta m \\ \delta Q &= -\frac{ua}{u-a}\,\delta(\log_e S) + \frac{a}{\gamma R}\,\delta\eta - \frac{a}{\rho S(u-a)}\,\delta m \end{aligned}\right\} \tag{15}$$

It should be pointed out that the quantity δm will itself have a positive or negative sign, depending upon the direction (upstream or downstream) which a characteristic crosses the point of mass removal. The quantity δm can also be expressed in the following form:

$$\delta m = \frac{\partial m}{\partial x}\,\Delta x \tag{16}$$

where $\partial m/\partial x$ is positive if mass is removed from the channel and Δx will be positive for the downstream direction.

The magnitude of the quantity δm can readily be evaluated by consideration of the equations of continuity and momentum referred to the dimension perpendicular to the channel. A simplification is possible, however, since the pressure rise across the shock wave, the pressure difference between the channel and the surge chamber, is generally sufficiently large so that the flow through the slits is choked. In this case, therefore,

$$|\delta m| = \rho^* a^* A \tag{17}$$

and the variation of P and Q, produced by mass removal only, reduces to

$$\left.\begin{aligned} |\delta P| &= \frac{a^2}{(u+a)}\,\frac{\rho^*}{\rho}\,\frac{a^*}{a}\,\frac{A}{S} \\ |\delta Q| &= \frac{a^2}{(u-a)}\,\frac{\rho^*}{\rho}\,\frac{a^*}{a}\,\frac{A}{S} \end{aligned}\right\} \tag{18}$$

In equation (18), the ambient stream quantities in the channel correspond to stagnation conditions with respect to the cross flow through the transverse slits. Consequently, the following ratios are constants:

$$\left.\begin{aligned} \frac{\rho^*}{\rho} &= 0.634 \\ \frac{a^*}{a} &= 0.913 \end{aligned}\right\} \tag{19}$$

The resultant magnitudes of P and Q, due to mass removal, and assuming the flow through the slits is choked, are

$$\left.\begin{aligned} |\delta P| &= 0.578 \frac{a^2}{(u + a)} \frac{A}{S} \\ |\delta Q| &= 0.578 \frac{a^2}{(u - a)} \frac{A}{S} \end{aligned}\right\} \tag{20}$$

The effects of shock waves and large entropy discontinuities are not included in the foregoing theoretical considerations. Both these effects were present in the analysis by the method of characteristics. A discussion of how these effects are handled is given in Appendix A.

In performing the characteristics analysis, it was also necessary to consider three types of interactions involving shock waves; namely,

1. Interaction of the pulse shock with the steady-flow normal shock

2. Interaction of the resultant shock with the flow out of the channel at the instant the shock crosses the transverse slits which open into the surge chamber

3. Interaction of the resultant shock with expansion waves from downstream which "catch up" with the shock and change its strength

The method of solution for each of these interactions consists of a series of successive approximations and is discussed in Appendix B.

APPLICATION TO PARTICULAR DESIGN

Preliminary Considerations

Shape of channel.- The method of characteristics as developed herein was used to study the stability of the steady-flow normal shock in a small double-throat supersonic wind tunnel equipped with a surge chamber. The contour of the channel is given in figure 1. The Mach numbers at the test section and the second throat were 1.64 and 1.42, respectively. The supersonic part of the channel was designed according to the steady-flow, two-dimensional method of characteristics. A diffusor half angle of 2° was used in order to minimize separation losses in the subsonic part of the flow. In the operating condition, the equilibrium position of the normal shock occurred 5.8 inches downstream from the first minimum section, that is, 1.3 inches downstream of the second throat and 0.3 inch downstream of the transverse slits. The Mach number immediately upstream of the normal shock was 1.55.

Construction of velocity profiles.- With the shape of the channel and the position of the normal shock now specified, the steady-flow velocity profile was computed and is shown in figure 2. The initial properties of a pulse originating downstream in the diffusor section are generally not known since they may arise from a variety of causes. It was shown in reference 1, however, that the velocity profile of a pulse takes a definite shape as it travels upstream, regardless of the conditions at its origin; the upstream section of a compression pulse will steepen to form a leading-edge shock, while the velocity profile of the expansion phase of the pulse behind this shock will assume a slope given by

$$\left(\frac{du}{dx}\right)_{pulse} = -\left(\frac{du}{dx}\right)_{steady\ flow}$$

All the disturbance pulses considered in this analysis are compression pulses having this shape of velocity profile. Two such pulses are shown in figure 2, superimposed on the steady-flow velocity profile at the position of impending intersection with the steady-flow normal shock.

Determination of initial flow conditions.- In order to start the characteristics analysis, the flow conditions, including the values of the characteristic quantities (eq. (9)) must be determined at all points in the channel at the time of the intersection of the pulse shock with the steady-flow normal shock. The details of this computation are given in Appendix C.

Analysis and Results

The method of characteristics was first applied to the channel, without mass removal, to find the "critical" pulse, that pulse which will supply sufficient energy to displace the normal shock to the unstable equilibrium position and, hence, unstart the flow. The order of magnitude of the critical pulse can be determined according to the methods of reference 1 where it was shown that, in the vicinity of Mach number 1, the velocity-profile area of the critical pulse[4] will be equal to the area between the steady-flow velocity profiles formed by the normal shock in the stable and unstable equilibrium positions (see fig. 2). This rule will, of course, give errors for Mach numbers greater than 1 but can be used as a first approximation. The present analysis, using the method of characteristics, showed that the critical pulse had a velocity-profile area about 68 percent of that given by reference 1. This result is in agreement with an investigation described in reference 6 which indicated a velocity-profile area of approximately 65 percent. The critical pulse is the smaller pulse shown in figure 2. A time-displacement history of the resultant shock formed by the interaction of the critical pulse with the steady-flow normal shock is given in figure 3.

It was decided, as an appropriate measure of the effectiveness of the surge chamber, to determine the size of transverse slit necessary to prevent unstarting of the flow by a pulse having a velocity-profile area double that of the critical pulse already determined. This double critical pulse is the larger pulse shown in figure 2. Figure 3 also presents time-displacement diagrams for the resultant shocks formed by the interaction of the steady-flow normal shock with the double critical pulse for the following conditions: no mass removal, 1/8-inch transverse slits, 1/4-inch transverse slits. It is evident that 1/4-inch slits are close to the smallest size which will dissipate the action of the double critical pulse.

In all cases, the pressure in the channel, at the point of mass removal, was sufficiently large to cause the mass flow into the surge chamber to be choked, thereby allowing the use of equation (19) to compute δP and δQ across the slits.

EXPERIMENT

Part of the experimental phase of this investigation consists in generating strong compression pulses in the flow and observing the interaction of the pulses with the steady-flow normal shock for the wind

[4]The velocity-profile area of a pulse is the area between the steady-flow velocity profile of the channel and the velocity profile imposed by the pulse.

tunnel in one of the two following operating conditions: (a) slits into surge chamber closed, no mass removal; and (b) slits into surge chamber open 1/4 inch. By means of a modified shock tube, it was possible to generate pulses having a velocity profile approximately the same as those used in the characteristics analysis. Hence, these experimental tests could parallel the analytical studies by determining the relative strengths of the strong pulses which would just unstart the flow under the stated operating conditions.

A further check on the effects of mass removal was made by operating the wind tunnel with the normal shock just downstream of the transverse slits and observing the effectiveness of the surge chamber in damping the movement of the shock caused by the incidence of small random disturbances. Since small random disturbances are encountered more often than strong pulses, it was felt that this test might be more representative of actual operating conditions.

Apparatus

Wind tunnel and optical system.- The experimental tests were carried out in a small intermittent supersonic wind tunnel in the gas dynamics laboratory of the Graduate School of Aeronautical Engineering, Cornell University. The width of the channel was 1 inch. The only modifications to the tunnel were the construction of new nozzle blocks, as shown in figure 1, and the construction of a bracket for mounting the pulse-generating device at the end of the diffusor. The transverse slits, which connect the channel to the surge chamber, were adjustable to allow an opening up to 1/2 inch. The surge chamber was designed to be large enough so that the pressure would not change appreciably within the length of time necessary for the shock to travel from the stable equilibrium position to the unstable equilibrium position and return.

The optical apparatus consisted of a schlieren system of conventional design and was provided with two light sources. A continuous light source was used for visual observation and also, in conjunction with a conventional camera shutter, for taking schlieren pictures with exposures of 1/25 second. The other light source, used for photography only, was a high-intensity spark having an effective duration of 1 microsecond.

Pulse tube.- The compression pulses were generated in a small shock tube which was mounted on the end of the diffusor. The shock tube, called a "pulse tube," differs from the conventional design, described in reference 7, in that the rearward wall of the high-pressure chamber is placed close to the diaphragm. The longitudinal dimensions are proportioned so that the front of the expansion wave reflected from the back wall just overtakes the shock at the forward end of the tube. At this instant the velocity distribution over the length of the tube decreases

almost linearly from a large negative value behind the shock to a very small positive value at the rear of the pulse. Figure 4 presents a typical analysis by the method of characteristics of the flow in the pulse tube together with a plot of the velocity profile. It will be recalled that the velocity profile of the compression pulses used in the theoretical analysis (see fig. 2) jumps discontinuously through a shock wave to a large negative value and then increases almost linearly to zero. Hence, the pulse tube generates a compression pulse with the correct shape of velocity profile needed to check the prediction of the theory.

The following dimensions of the pulse velocity profile are required: (a) the velocity discontinuity at the shock front, and (b) the velocity-profile area. The velocity discontinuity at the shock front of the pulse is determined by the initial pressure ratio across the diaphragm. The area of the pulse can be adjusted to the required value by changing the over-all length of the pulse tube. The pulse tube can be designed to give precisely the required velocity-profile area corresponding to only one particular value of the velocity discontinuity at the shock front. At other values of velocity discontinuity, the profile area obtained in the pulse tube will differ slightly from the profile area required in the theoretical analysis. This difference, however, was found to be less than 4 percent throughout the range of values employed in the experiment.

The pulse tube was designed according to the dimensions of the double critical pulse shown in figure 2. This pulse had a velocity discontinuity, $\Delta u/a_o$, across the shock front of 0.515 and a velocity-profile area of 1.57 (units of $u/a_o \times$ inches). It was anticipated, however, that there would be losses in pulse strength caused by the pulse traversing the gap between the end of the pulse tube and the end of the diffusor, as well as losses resulting from the separated flow in the diffusor. It was estimated that these losses would cause a reduction in the over-all pulse velocity profile of 20 percent. For purposes of design, therefore, the dimensions of the double critical pulse were increased by 20 percent which brought the velocity-profile area to a value of 1.90 (units of $u/a_o \times$ inches) and a leading-edge velocity discontinuity, $\Delta u/a_o$, of 0.610. Two additional analyses were carried out for weaker pulses. From these analyses the relation was determined between the velocity-profile area and initial pressure in the high-pressure chamber of the pulse tube. The graph of this relation is presented in figure 5.

Figure 6 shows the entire test setup with the pulse tube in its operating position at the end of the channel. A larger photograph of the pulse tube is shown in figure 7. Also shown in figure 7 is the diaphragm rupture mechanism which consisted of a needle attached to a solenoid switch. Closing the circuit of the solenoid switch caused the needle to be displaced inward, thus rupturing the diaphragm. Due to the deflection of the diaphragm under pressure, a filler plate was attached to the back wall of the high-pressure chamber (see fig. 8). The size of this plate

was approximately equal to the added volume caused by the diaphragm deflection and, consequently, acted to keep the pulse size closer to that dictated by the theoretical design.

Procedure

In order to study the effect of mass removal against the action of the compression pulses from the pulse tube, tests were conducted with the transverse slits 1/4 inch open and were repeated with slits closed. The procedure in both cases was to fill the high-pressure chamber in the pulse tube to a desired pressure, then start the wind tunnel and bring the normal shock to its proper position downstream of the second throat. The diaphragm of the pulse tube was then punctured. The effect of the interaction of the compression pulse with the steady-flow normal shock was observed on the schlieren screen: Either the normal shock returned to its stable equilibrium position downstream of the second throat or was driven to the secondary stable equilibrium position upstream of the test section. These tests were repeated with different values of pulse-tube pressure until that pressure corresponding to the critical pulse was determined.

In order to determine the effect of mass removal against the action of small random disturbances, a second series of tests was carried out with the air flow from the end of the diffusor partially blocked. The sharp diversion of air at this point created random pressure variations which were propagated upstream through the diffusor. It was felt that the disturbance level created in this manner would correspond roughly to disturbances produced by the exhaust system of an actual wind tunnel. For this part of the experiment, the normal shock was placed in a position at the downstream edge of the transverse slits. The effect of mass removal to the surge chamber was observed by comparing the oscillation of the normal shock when the slits were 1/4 inch open with the oscillations present when the slits were closed. An attempt was made to show this effect by taking schlieren photographs with a spark (1-microsecond exposure) and with an exposure of 1/25 second. The normal shock wave was photographed at both these exposures, first with the slits open 1/4 inch and then with the slits closed. If mass removal is effective in damping oscillations of the shock wave, there will be a close similarity between the 1/25-second and 1-microsecond exposures.

RESULTS AND DISCUSSION

The experimental tests to determine the effect of mass removal against the action of strong compression pulses revealed that the pulse necessary to unstart the tunnel with 1/4-inch transverse slits was

produced by a pulse-tube-chamber pressure of approximately 62 psi gage. With the transverse slits closed, the pulse necessary to unstart the tunnel was produced by a pressure of about 28 psi gage. As shown in figure 5, the velocity-profile areas corresponding to these pressures are 1.80 and 0.87, respectively. The velocity-profile area of the pulse required to unstart the tunnel with 1/4-inch slits is approximately double the area required with slits closed. This result is in agreement with the theoretical analysis, as shown in figure 3, which predicts that the action of the double critical pulse will be dissipated by mass removal through 1/4-inch transverse slits.

The second series of tests demonstrated the effect of mass removal against the action of small random disturbances. With the slits open 1/4 inch, the normal shock was never driven upstream by the random disturbances, and a marked decrease in the oscillation of the normal shock was noted as compared with the oscillations present when the slits were closed.

Schlieren photographs, with exposure times of 1/25 second and 1 microsecond, were taken with the transverse slits both closed and open and are presented in figures 9 and 10, respectively. The oscillatory motion of the normal shock, caused by the random disturbances, can be observed in figure 9 by noting the difference in clarity between the photographs taken at the two exposure times. The effect of mass removal in damping these oscillations is to be observed by comparing the relative clarity between the 1/25-second exposures of figures 9 and 10 and, also, by noting the similarity between the 1/25-second and 1-microsecond exposures of figure 10.

When taking schlieren photographs, the shock could not be positioned visually because the visual screen was blocked by the photographic plate holder. An approximate shock position was fixed by reference to the settling chamber pressure. Under these conditions it was difficult to photograph the normal shock at a desired average position. As a result of this difficulty, the photographs of figure 10 show the normal shock at an average position farther downstream from the transverse slits than was desired. Although some damping is indicated by the relative clarity of the 1/25-second exposure in figure 10, as compared to the 1-microsecond exposure, the effect is not as striking as was observed visually.

CONCLUDING REMARKS

In order to stabilize normal shock waves in channel flow against the effect of disturbances originating downstream, a method based on mass removal from the channel by means of a surge chamber was developed at Cornell University. The stabilizing action is initiated by the motion of the steady-flow normal shock caused by the disturbances and requires the use of no additional power facilities.

With the use of the method of characteristics (extended to include mass removal at a point in the channel), the flow was analyzed in a channel shape similar to that used in a double-throat supersonic wind tunnel. It was found that the mass-removal technique was effective in damping the motion of the normal shock wave produced by strong compression disturbances.

To check the findings of the theoretical analysis, a series of experimental tests was performed in a small double-throat wind tunnel into which compression disturbances of known strength were introduced by a pulse generating device. The experimental results were in quantitative agreement with the results of the theoretical analysis. An additional series of experimental tests was performed in which it was found that the mass-removal technique was effective in damping the oscillatory motion of the steady-flow normal shock caused by small random disturbances.

From the theoretical and experimental results, it can be concluded, therefore, that the mass-removal technique is effective in stabilizing normal shock waves against compression disturbances originating downstream, and that the performance can be accurately computed by the method of characteristics.

Ames Aeronautical Laboratory
National Advisory Committee for Aeronautics
Moffett Field, Calif., Mar. 31, 1953

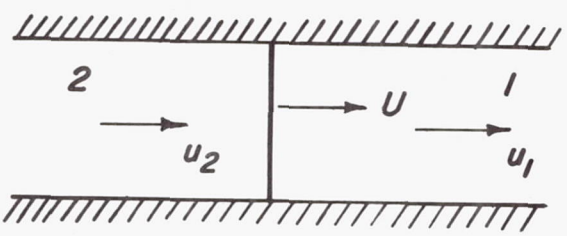
APPENDIX A

APPLICATION OF THE METHOD OF CHARACTERISTICS ACROSS STRONG DISCONTINUITIES

Normal Shock Waves

The change in each of the characteristic quantities, P and Q, and the entropy, η, across a normal shock wave may be computed using the customary Rankine-Hugoniot relations. However, in the construction of characteristic diagrams where solutions across shock waves are required many times, it has proved convenient to prepare two auxiliary charts to facilitate these computations. To begin with, it is desirable to define the two classes of shock waves. A P shock is defined simply as a shock wave which, on a time-displacement diagram, is moving to the right relative to the fluid. Conversely, a Q shock is a shock wave that moves to the left relative to the fluid. In addition, all velocities are taken to be positive for movement from left to right and negative from right to left.

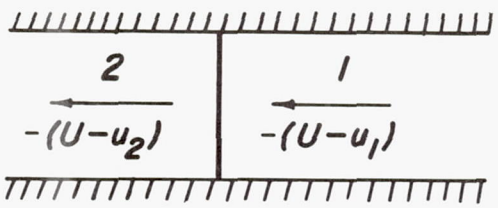
The first of these auxiliary charts expresses the change across a shock wave in the quantity P in terms of the corresponding change in Q. Consider a P shock in channel flow as shown in sketch (A1). The changes in the characteristic quantities, expressed in non-dimensional form by dividing by the speed of sound, a_1, is



Sketch (A1)

$$\left(\frac{P_2 - P_1}{a_1}\right)_P = \frac{\frac{2c_v}{R} a_2 + u_2 - \frac{2c_v}{R} a_1 - u_1}{a_1}$$

$$\left(\frac{Q_2 - Q_1}{a_1}\right)_P = \frac{\frac{2c_v}{R} a_2 - u_2 - \frac{2c_v}{R} a_1 + u_1}{a_1} \qquad \text{(A1)}$$



Sketch (A2)

Upon transferring to a coordinate system moving with the normal shock, as shown in sketch (A2), it is found that the relations given in equation (A1) now become

$$\left.\begin{aligned}\left(\frac{P_2 - P_1}{a_1}\right)_P &= \frac{\frac{2c_v}{R}a_2 - (U - u_2) - \frac{2c_v}{R}a_1 + (U - u_1)}{a_1} \\ \left(\frac{Q_2 - Q_1}{a_1}\right)_P &= \frac{\frac{2c_v}{R}a_2 + (U - u_2) - \frac{2c_v}{R}a_1 - (U - u_1)}{a_1}\end{aligned}\right\} \quad (A2)$$

Equation (A2) is essentially unchanged from equation (A1) since it merely involves the addition and subtraction of the shock velocity, U, in the numerator of the right side. This observation serves to illustrate the fact that $(P_2-P_1)/a_1$ and $(Q_2-Q_1)/a_1$ are independent of coordinate system. Equation (A2) may be brought into the following form:

$$\left.\begin{aligned}\left(\frac{P_2 - P_1}{a_1}\right)_P &= \frac{a_2}{a_1}\left(\frac{2c_v}{R} - \frac{U - u_2}{a_2}\right) - \left(\frac{2c_v}{R} - \frac{U - u_1}{a_1}\right) \\ \left(\frac{Q_2 - Q_1}{a_1}\right)_P &= \frac{a_2}{a_1}\left(\frac{2c_v}{R} + \frac{U - u_2}{a_2}\right) - \left(\frac{2c_v}{R} + \frac{U - u_1}{a_1}\right)\end{aligned}\right\} \quad (A3)$$

In terms of quantities listed in the standard steady-flow normal-shock table,

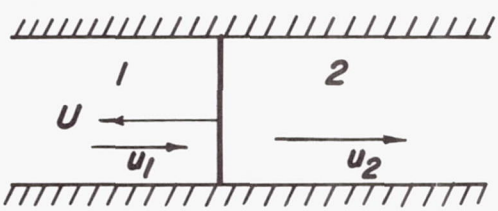
$$\left.\begin{aligned}M_{s_1} &= \frac{U - u_1}{a_1} \\ M_{s_2} &= \frac{U - u_2}{a_2}\end{aligned}\right\} \quad (A4)$$

Equations (A3) then becomes

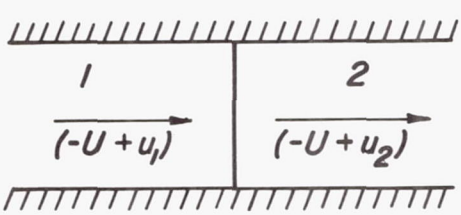
$$\left.\begin{aligned}\left(\frac{P_2 - P_1}{a_1}\right)_P &= \frac{a_2}{a_1}\left(\frac{2c_v}{R} - M_{s_2}\right) - \left(\frac{2c_v}{R} - M_{s_1}\right)\\ \left(\frac{Q_2 - Q_1}{a_1}\right)_P &= \frac{a_2}{a_1}\left(\frac{2c_v}{R} + M_{s_2}\right) - \left(\frac{2c_v}{R} + M_{s_1}\right)\end{aligned}\right\} \quad (A5)$$

With reference to any of the standard steady-flow normal-shock tables, the chart of $(P_2-P_1)/a_1$ as a function of $(Q_2-Q_1)/a_1$ can be constructed.

For comparison, a Q shock in channel flow would be represented as in sketch (A3). Upon transformation to a coordinate system moving with the shock velocity, U, the flow would be represented as in sketch (A4). The change in the characteristic quantities for the case of the Q shock would now be



Sketch (A3)



Sketch (A4)

$$\left.\begin{aligned}\left(\frac{P_2 - P_1}{a_1}\right)_Q &= \frac{a_2}{a_1}\left(\frac{2c_v}{R} + \frac{-U+u_2}{a_2}\right) - \left(\frac{2c_v}{R} + \frac{-U+u_1}{a_1}\right)\\ \left(\frac{Q_2 - Q_1}{a_1}\right)_Q &= \frac{a_2}{a_1}\left(\frac{2c_v}{R} - \frac{-U+u_2}{a_2}\right) - \left(\frac{2c_v}{R} - \frac{-U+u_1}{a_1}\right)\end{aligned}\right\} \quad (A6)$$

In terms of quantities listed in standard steady-flow normal-shock tables

$$\left.\begin{aligned} M_{s_1} &= \frac{-U + u_1}{a_1} \\ M_{s_2} &= \frac{-U + u_2}{a_2} \end{aligned}\right\} \tag{A7}$$

and equations (A6) then become

$$\left.\begin{aligned} \left(\frac{P_2 - P_1}{a_1}\right)_Q &= \frac{a_2}{a_1}\left(\frac{2c_v}{R} + M_{s_2}\right) - \left(\frac{2c_v}{R} + M_{s_1}\right) \\ \left(\frac{Q_2 - Q_1}{a_1}\right)_Q &= \frac{a_2}{a_1}\left(\frac{2c_v}{R} - M_{s_2}\right) - \left(\frac{2c_v}{R} - M_{s_1}\right) \end{aligned}\right\} \tag{A8}$$

Comparing equations (A8) with the corresponding equation for the P shock, the following rule can be stated:

$$\left.\begin{aligned} \left(\frac{P_2 - P_1}{a_1}\right)_P &= \left(\frac{Q_2 - Q_1}{a_1}\right)_Q \\ \left(\frac{Q_2 - Q_1}{a_1}\right)_P &= \left(\frac{P_2 - P_1}{a_1}\right)_Q \end{aligned}\right\} \tag{A9}$$

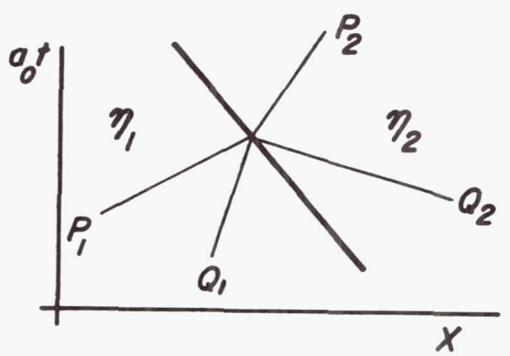
The curves of $(P_2-P_1)/a_1$ as a function of $(Q_2-Q_1)/a_1$ for a P shock can, therefore, be used for Q shocks by merely interchanging the ordinate and abscissa.

The second of the necessary charts concerns the entropy change across a normal shock. The following relation expresses the entropy change between any two equilibrium conditions of a perfect gas.

$$\frac{\eta_2 - \eta_1}{\gamma R} = \frac{2c_p}{\gamma R} \log_e\left(\frac{a_2}{a_1}\right) - \frac{1}{\gamma} \log_e\left(\frac{p_2}{p_1}\right) \qquad \text{(A10)}$$

For a normal shock, however, the ratios a_2/a_1 and p_2/p_1 are related through the Rankine-Hugoniot equations. With the use of a standard set of steady-flow normal-shock tables, it is therefore possible to compute $(\eta_2-\eta_1)/\gamma R$ as a function of a_2/a_1 only.

In applying the method of characteristics across a normal shock wave, a complete solution involves a knowledge of the six quantities as shown in sketch (A5). In the present analysis, which is concerned only with Q shocks, the quantities P_1, Q_1, Q_2, and η_1 are known, either from boundary conditions or from previous computations. With the aid of the chart of $(P_2-P_1)/a_1$ as a function of $(Q_2-Q_1)/a_1$, the value of P_2 can be determined. According to the definitions of P and Q, the flow velocity and speed of sound may be computed from the following general relation:



Sketch (A5)

$$\left.\begin{aligned} a &= \frac{P + Q}{4c_v/R} \\ u &= \frac{P - Q}{2} \end{aligned}\right\} \qquad \text{(A11)}$$

With the value of a_2/a_1 now known, η_2 can be determined from the chart of $(\eta_2-\eta_1)/\gamma R$ as a function of a_2/a_1.

Strong Entropy Discontinuities

When a large entropy discontinuity exists in a fluid, the pressures and velocities on each side of the interface are identical. For this condition, equation (A10) becomes

$$\frac{\eta_2 - \eta_1}{\gamma R} = \frac{2c_p}{\gamma R} \log_e \left(\frac{a_2}{a_1}\right) \tag{A12}$$

from which the speed-of-sound ratio between conditions on each side of the interface is

$$\frac{a_2}{a_1} = e^{\frac{\eta_2 - \eta_1}{2c_p}} \tag{A13}$$

Since the velocities on either side of the interface are constant, the difference between the characteristic quantity P across the entropy discontinuity is expressed as

$$P_2 - P_1 = \frac{2c_v}{R}(a_2 - a_1) = \frac{2c_v}{R} a_1 \left(\frac{a_2}{a_1} - 1\right) \tag{A14}$$

Substitution of the expression for the speed-of-sound ratio in equation (A13) into equation (A14) gives the following relation:

$$P_2 - P_1 = \frac{2c_v}{R} a_1 \left(e^{\frac{\eta_2 - \eta_1}{2c_p}} - 1\right) \tag{A15}$$

By a procedure analogous to that used in obtaining equation (A15), the following expression can be written for conditions across the interface:

$$P_1 + Q_2 = 2 \frac{c_v}{R} a_1 \left(e^{\frac{\eta_2 - \eta_1}{2c_p}} + 1 \right) \tag{A16}$$

Combining equations (A15) and (A16) yields

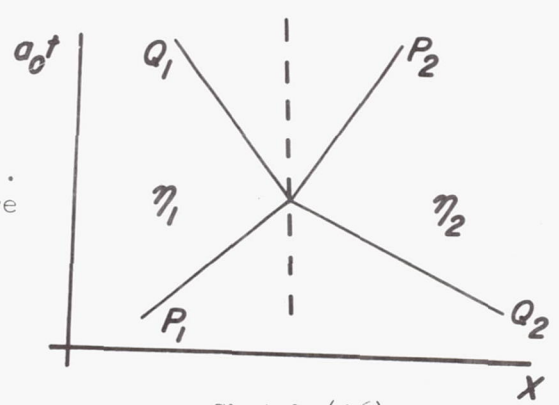
$$\left.\begin{aligned} P_2 - P_1 &= (P_1 + Q_2) \left[\frac{e^{\frac{\eta_2 - \eta_1}{2c_p}} - 1}{e^{\frac{\eta_2 - \eta_1}{2c_p}} + 1} \right] \\ \text{or} \\ P_2 - P_1 &= (P_1 + Q_2) \tanh \frac{\eta_2 - \eta_1}{4c_p} \end{aligned}\right\} \tag{A17}$$

By a similar procedure to that used in obtaining equation (A17), the following expression can be obtained:

$$Q_2 - Q_1 = (Q_1 + P_2) \tanh \frac{\eta_2 - \eta_1}{4c_p} \tag{A18}$$

For very small entropy discontinuities, the first term of the series expansion for the hyperbolic tangent may be sufficient, and equations (A17) and (A18) reduce to the form given in equation (15) in the text of this report.

The application of equations (A17) and (A18) to the determination of the flow quantities across a typical strong entropy discontinuity can be shown with reference to sketch (A6). The quantities P_1, Q_2, η_1, and η_2 are known from boundary conditions. The problem is to determine Q_1 and P_2. From equations (A17) and (A18), the values of $(P_2 - P_1)$ and $(Q_2 - Q_1)$ can be computed from known conditions. Q_1 and P_2 can then be computed since Q_2 and P_1 are known.



Sketch (A6)

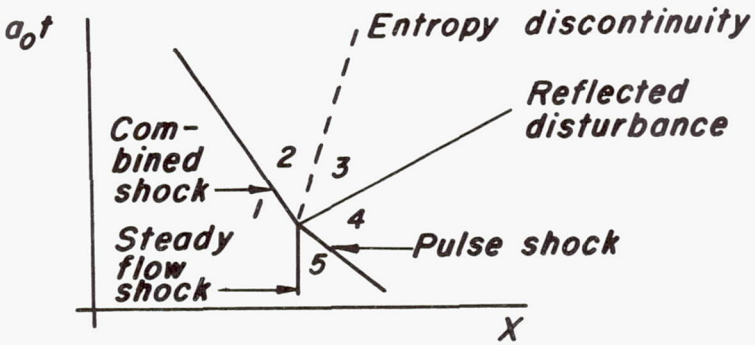
APPENDIX B

TYPICAL INTERACTIONS

The theory of wave interactions is discussed in reference 5. However, the solution of any actual interaction process requires a procedure for numerical computation, and this aspect of the problem is hardly touched upon elsewhere in the literature. Accordingly, an attempt is made here to present a practical method of solution for those interactions encountered in the present analyses.

Interaction of Two Q Shock Waves

This interaction is encountered when the shock wave at the leading edge of the compression pulse encounters the steady-flow normal shock. A schematic diagram of this interaction is given in sketch (B1). The interaction of the two shock waves results in (1) a single strong shock wave which moves upstream with a velocity intermediate to the interacting shocks; (2) a strong entropy discontinuity which moves downstream with the velocity of the fluid; and (3) a weak reflected disturbance which, as shown in reference 5, will be a rarefaction wave. The method for solution is given in the following outline form:



Sketch (B1)

Given:

1. All conditions (P, Q, u, a, η) in sectors 1, 4, 5.
2. Velocity is constant across entropy discontinuity: $u_2 = u_3$.
3. Q and η are constant across the reflected disturbance. $Q_3 = Q_4$, $\eta_3 = \eta_4$.

Find:

1. All conditions (P, Q, u, a, η) in sectors 2 and 3.
2. The velocity of the combined shock.

Auxiliary Charts (See Appendix A)

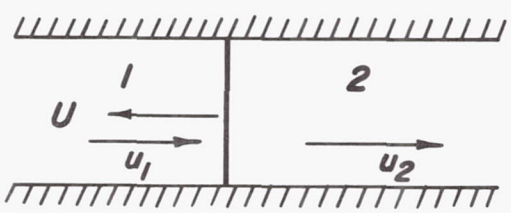
1. $(P_2-P_1)/a_1$ vs $(Q_2-Q_1)/a_1$ for Q shock.
2. $(\eta_2-\eta_1)/\gamma R$ vs $\frac{a_2}{a_1}$ for normal shock.
3. Steady-flow normal-shock tables.

Procedure:

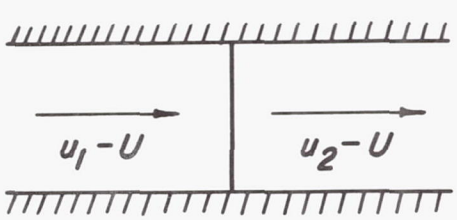
1. Assume $(Q_2-Q_1)/a_1$.
2. Obtain $(P_2-P_1)/a_1$ from charts of $(P_2-P_1)/a_1$ vs $(Q_2-Q_1)/a_1$ for Q shock.
3. Compute P_2, Q_2, u_2, a_2.
4. Obtain η_2 from chart of $(\eta_2-\eta_1)/\gamma R$ vs $\frac{a_2}{a_1}$ for normal shock.
5. Compute $(Q_3 - Q_2)$ from equation (A18). In equation (A18) replace subscript 1 by subscript 3, and use the given value of Q_3 in computing the factor $(Q_3 + P_2)$.
6. Compare Q_3 (computed) with Q_3 (given) and repeat steps 1 through 5 until these quantities are equal.
7. Compute P_3 from equation (A17) replacing the subscripts as indicated in step 5.
8. With Q_3 from step 6 and P_3 from step 7, compute u_3 and a_3 with the use of equation (A11).

With conditions in sectors 1 and 2 now known, the velocity of the resultant shock can now be computed. Consider the motion of this shock as shown in sketch (B2). When transformed to a coordinate system moving with the velocity of the shock, the picture then assumes the form shown in sketch (B3). The Rankine-Hugoniot relations may be used with reference to this latter sketch. As such,

$$\left.\begin{aligned} U &= u_1 - M_{s_1} a_1 \\ U &= u_2 - M_{s_2} a_2 \end{aligned}\right\} \quad (B1)$$



Sketch (B2)



Sketch (B3)

The velocity of the shock U may be determined from either of the equations (B1) with the aid of a set of steady-flow normal-shock tables.

A numerical example of this procedure may help. In practice it is found convenient to express all velocities, and also P and Q, as multiples of a standard velocity. In this case the standard velocity is taken as the standard speed of sound, a_o (1120 ft/sec), and the values of u, a, P, and Q listed are actually u/a_o, a/a_o, P/a_o, and Q/a_o. The following initial conditions are given in sectors 1, 4, and 5:

$$P_1 = 5.384 \quad u_1 = 1.274 \qquad \frac{\eta_1}{\gamma R} = 0$$

$$Q_1 = 2.836 \quad a_1 = 0.822$$

$$P_5 = 5.384 \quad u_5 = 0.654 \qquad \frac{\eta_5}{\gamma R} = 0.069$$

$$Q_5 = 4.131 \quad a_5 = 0.957$$

$$P_4 = 5.450 \quad u_4 = 0.290 \qquad \frac{\eta_4}{\gamma R} = 0.079$$

$$Q_4 = 4.870 \quad a_4 = 1.034$$

$$\frac{\eta_3}{\gamma R} = \frac{\eta_4}{\gamma R} = 0.079$$

$$Q_3 = Q_4 = 4.870$$

Following the specified procedure, the resulting solution is

1. Assume $(Q_2-Q_1)/a_1 = 2.648$
2. Obtain $(P_2-P_1)/a_1 - 0.227$ from chart of $(Q_2-Q_1)/a_1$ vs $(P_2-P_1)/a_1$
3. Compute $P_2 = 5.571 \quad u_2 = 0.280$

   $Q_2 = 5.011 \quad a_2 = 1.058$
4. $a_2/a_1 = 1.288$, hence $(\eta_2 - \eta_1)/\gamma R = \eta_2/\gamma R = 0.212$ from chart of $\Delta\eta/\gamma R$ vs a_2/a_1

5. $(\eta_3-\eta_2)/\gamma R = 0.133 \quad (\eta_3-\eta_2)/4c_p = 0.0133$

$\tanh (\eta_3-\eta_2)/4c_p = 0.0133$

$Q_3 + P_2 = 10.441 \quad$ Use Q_3 (given)

$Q_2 - Q_3 = 0.139$

6. $Q_8 = 4.871$ (computed) as compared to

$Q_3 = 4.870$ (given)

7. $P_3 = 4.432$

$u_3 = 0.280$

$a_3 = 0.930$

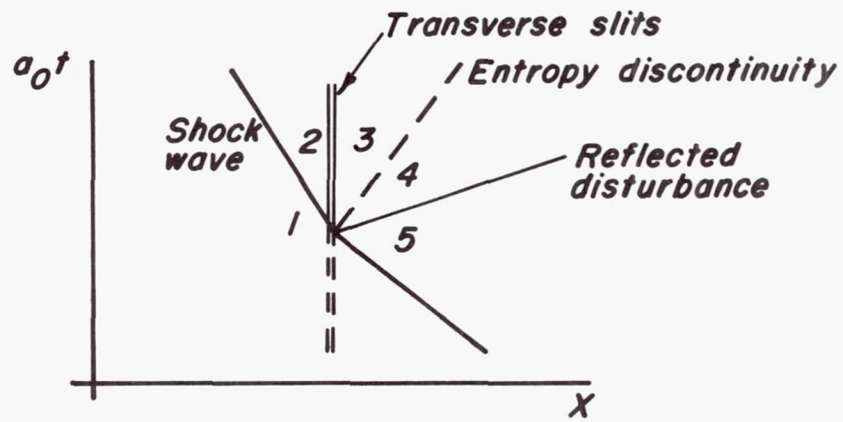
8. From $\frac{a_2}{a_1} = 1.288$, $M_{s_1} = 1.966$ and $M_{s_2} = 0.583$

as found in shock tables

From equation (B1) $U = -0.340$

Shock Wave Crossing Transverse Slits

A schematic diagram of this interaction is given in sketch (B4).



Sketch (B4)

As shown here, the resultant shock moves upstream and crosses the slits. The pressure difference between the channel and the surge chamber causes fluid to flow out of the channel through the transverse slits. This mass removal results in an immediate expansion which interacts with the shock wave and reduces its strength and velocity. The change in strength of

the shock wave introduces an entropy discontinuity into the fluid, as well as a small reflected disturbance. The method of solution for this interaction is given in the following outline form:

Given:

1. All conditions (P, Q, u, a, η) in sectors 1 and 5.

2. Velocity is constant across entropy discontinuity: $u_2 = u_3$.

3. Q and η are constant across the reflected disturbance: $\eta_4 = \eta_5$ and $Q_4 = Q_5$. It should be pointed out here that if this reflected disturbance should be a compression wave, then the invariance of η and Q from sector 4 to 5 will not be strictly valid. Inasmuch as the disturbance is extremely weak, however, the variation of η and Q is so small that, to the accuracy of this analysis, it cannot be detected.

4. Dimensions of the transverse slits.

Find:

1. All conditions (P, Q, u, a, η) in sectors 2, 3, and 4.

2. The velocity of the shock after it has crossed the transverse slits.

Auxiliary charts necessary (See Appendix A):

1. $(P_2-P_1)/a_1$ vs $(Q_2-Q_1)/a_1$ for normal shock.

2. $(\eta_2-\eta_1)/\gamma R$ vs a_2/a_1 for normal shock.

3. Steady-flow normal-shock tables.

Procedure:

1. Assume $(Q_2-Q_1)/a_1$.

2. Obtain $(P_2-P_1)/a_1$ from chart.

3. Compute P_2, Q_2, u_2, a_2.

4. Obtain $\eta_2 = \eta_3$ from chart.

5. With the aid of equations (15) and (20), compute P_3, Q_3, u_3, and a_3. Since the average values of the speed of sound and flow velocity must be used, an iterative procedure is necessary to perform this step. This iteration can be performed best by first using $\bar{u} = u_2$ and $\bar{a} = a_2$. From the values of u_3 and a_3 thus

computed, new values of u and a can be computed. Repeat this process until sufficient accuracy is obtained.

6. Compute $(Q_3 - Q_4)$ from equation (A18) replacing subscript 1 by subscript 4 and subscript 2 by subscript 3. Use the given value of Q_4 in computing the factor $(Q_4 + P_3)$.

7. Compare Q_4(computed) with Q_3(given) and repeat steps 1 through 6 until these quantities are equal.

8. Compute P_4 from equation (A17) replacing the subscripts as indicated in step 6. Use Q_4 from step 7 to compute u_3, a_3.

9. Compute the speed of the shock after crossing the transverse slits using equation (B1).

A numerical example of this procedure is presented with 1/8-inch transverse slits on both the top and bottom of the channel and the following conditions given in sectors 1 and 5:

$$P_1 = 5.384 \quad u_1 = 1.274$$
$$Q_1 = 2.836 \quad a_1 = 0.822$$
$$\frac{\eta_1}{\gamma R} = 0$$

$$P_5 = 5.571 \quad u_5 = 0.280$$
$$Q_5 = 5.011 \quad a_5 = 1.058$$
$$\frac{\eta_5}{\gamma R} = 0.212$$

Following the specified procedure,

1. Assume $(Q_2-Q_1)/a_1 = 2.368$.

2. Obtain $(P_2-P_1)/a_1 = 0.177$ from chart.

3. Compute $P_2 = 5.529 \quad u_2 = 0.372$

   $Q_2 = 4.784 \quad a_2 = 1.031$

4. From $a_2/a_1 = 1.255 \quad (\eta_2-\eta_1)/\gamma R = \eta_2/\gamma R = \eta_3/\gamma R = 0.165$

5. By iterative procedure

   $$Q_3 - Q_2 = 0.179$$
   $$P_3 - P_2 = -0.096$$

and

$P_3 = 5.433 \quad u_3 = 0.235$

$Q_3 = 4.963 \quad a_3 = 1.040$

6. $(\eta_4\ \eta_3)/\gamma R = 0.047 \quad (\eta_4-\eta_3)/4c_p = 0.0047$

$\tanh\ (\eta_4-\eta_3)/4c_p = 0.0047$

$Q_4 + P_3 = 5.011 + 5.433 = 10.444$ Use Q_4 (given)

$(Q_4 - Q_3) = (P_4 - P_3) = 0.049$

7. $Q_4 = 5.012$ (computed) as compared to

$Q_4 = 5.011$ (given)

8. $P_4 = 5.484$

$u_4 = 0.235$

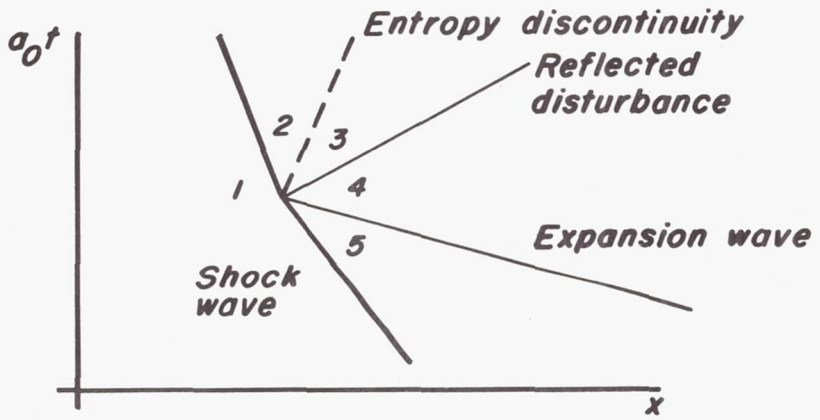
$a_4 = 1.050$

9. Using $\frac{a_2}{a_1} = 1.255$, obtain $M_{s_1} = 1.857$ and $M_{s_2} = 0.604$ from shock tables. From equation (B1) $U = -0.251$

Expansion Wave Overtaking Shock Wave

The leading-edge shock wave of the strong compression pulse is followed by an extended expansion zone. This expansion zone propagates upstream more rapidly than the shock and, hence, overtakes and weakens the shock. The process is actually a continuous one but, in applying the method of characteristics, the expansion zone is considered to be built up stepwise from a series of expansion waves.

A diagram of this process is shown in sketch (B5). The overtaking expansion wave interacts with the shock wave and reduces its strength



Sketch (B5)

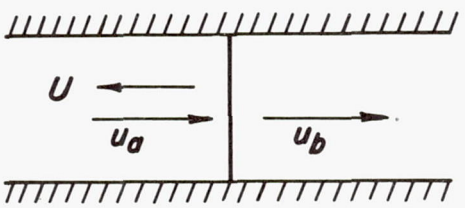
and velocity. The change in strength of the shock wave introduces an entropy discontinuity into the fluid, as well as a small reflected disturbance. The method of solution for this interaction is identical to that presented previously for the interaction of two Q shock waves.

APPENDIX C

DETERMINATION OF THE INTIAL VALUES OF THE CHARACTERISTIC QUANTITIES

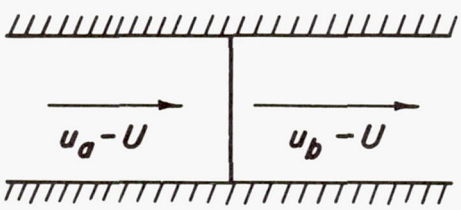
The velocity profile for a given pulse has been superimposed upon the steady-flow velocity profile at the time of impending interaction of the pulse shock with the steady-flow normal shock. Since the conditions in the region upstream of the disturbance pulse are unchanged by the presence of the pulse, the speed of sound and all other properties of the fluid in this region are known from the steady-flow conditions. It remains necessary, therefore, to evaluate only the speed of sound throughout the region downstream of the pulse shock. With the velocity profile of the channel already known, the characteristic quantities can then be calculated from equation (9).

The following procedure can be used to determine the speed of sound a_b immediately downstream of the pulse shock: Let sketch (C1) represent the flow conditions in the neighborhood of the upstream edge of the pulse.



Sketch (C1)

Superimpose a velocity -U on the flow field, thus converting to a coordinate system which represents velocities relative to the upstream edge of the pulse as shown in sketch (C2). The local speeds of sound, a_a and a_b, as well as the ambient pressure, temperature, and entropy, are independent of coordinate system and remain unchanged. With reference to sketch (C2), the following relations can be obtained:



Sketch (C2)

$$\left.\begin{aligned} \frac{u_a - U}{a_a} &= M_{s_a} \\ \frac{u_b - U}{a_b} &= M_{s_b} \end{aligned}\right\} \qquad (C1)$$

Equations (C1) can be combined to give

$$\frac{u_a - u_b}{a_a} = M_{s_a} - M_{s_b}\frac{a_b}{a_a} \qquad (C2)$$

which expresses conditions across a stationary normal shock. Since u_a, u_b, a_a, and p_a are already known, the quantities a_b, M_{s_a}, and M_{s_b} can be determined from equation (C2) by a trial and error calculation with the use of any of the standard tables for flow across a normal shock. The solution to equation (C2) will also determine the pressure ratio across the shock from which the value of p_b can be computed. From the integrated form of equation (4), namely,

$$\Delta\eta \Big|_a^b = 2c_p\left(\log_e \frac{a_b}{a_a}\right) - R\left(\log_e \frac{p_b}{p_a}\right) \qquad (C3)$$

the value of η_b can also be determined.

To compute the speed of sound at all points downstream of the pulse shock, the following assumptions were made:

1. The entropy is constant from the rear of the pulse shock, station b, to the end of the channel.

2. The pressure at the end of the pulse, p_c, is the same as the steady-flow pressure at that point.

3. The speed of sound along the pulse varies linearly with the flow velocity.

From assumption (1), the expression for the entropy change between stations b and c is

$$\Delta\eta \Big|_b^c = 2c_p\left(\log_e \frac{a_c}{a_b}\right) - R\left(\log_e \frac{p_c}{p_b}\right) = 0 \qquad (C4)$$

By assumption (2) and equation (C4), the speed of sound at the rear of the pulse, a_c, can be determined since a_b and p_b are known. With the velocity profile of the channel already known, assumption (3) permits an evaluation of the speed of sound at all points along the pulse. The values of the characteristic quantities, P and Q, (eq. (9)) can now be evaluated at all points in the channel at the time of impending intersection of the pulse shock with the steady-flow normal shock.

REFERENCES

1. Kantrowitz, A. R.: The Formation and Stability of Normal Shock Waves in Channel Flows. NACA TN 1225, 1947.

2. Riemann, B.: Uber die Fortpflunzung ebener Luftwellen von endlicher Schwingungsweite. Abhandlungen der Gesellschaft der Wissenschaften zu Gottingen, Mathematish-physikalische Klasse 8, p 43, 1858-59.

3. Kantrowitz, A. R.: Heat Engines Based on Wave Processes. Paper presented before the Annual Meeting of the A.S.M.E., Nov. 1948.

4. Kahane, A., and Lees, Lester: Unsteady One-Dimensional Flows with Heat Addition or Entropy Gradients.. Jour. Aero. Sci., vol. 15, no. 11, 1948.

5. Courant, R., and Friedricks, K. O.: Supersonic Flow and Shock Waves. Interscience Publishers, New York, 1948.

6. Kantrowitz, A. R., McDonald, E. E., and Perry, R.: The Response of a Normal Shock in a Channel Flow to Small Disturbances Coming from the Rear of the Channel. Cornell University Graduate School of Aeronautical Engineering, April 1949.

7. Hertzberg, A.: An Experimental Investigation of Two-Dimensional Non-Steady Shock Wave Phenomena. Cornell University Graduate School of Aeronautical Engineering, Sept. 1949.

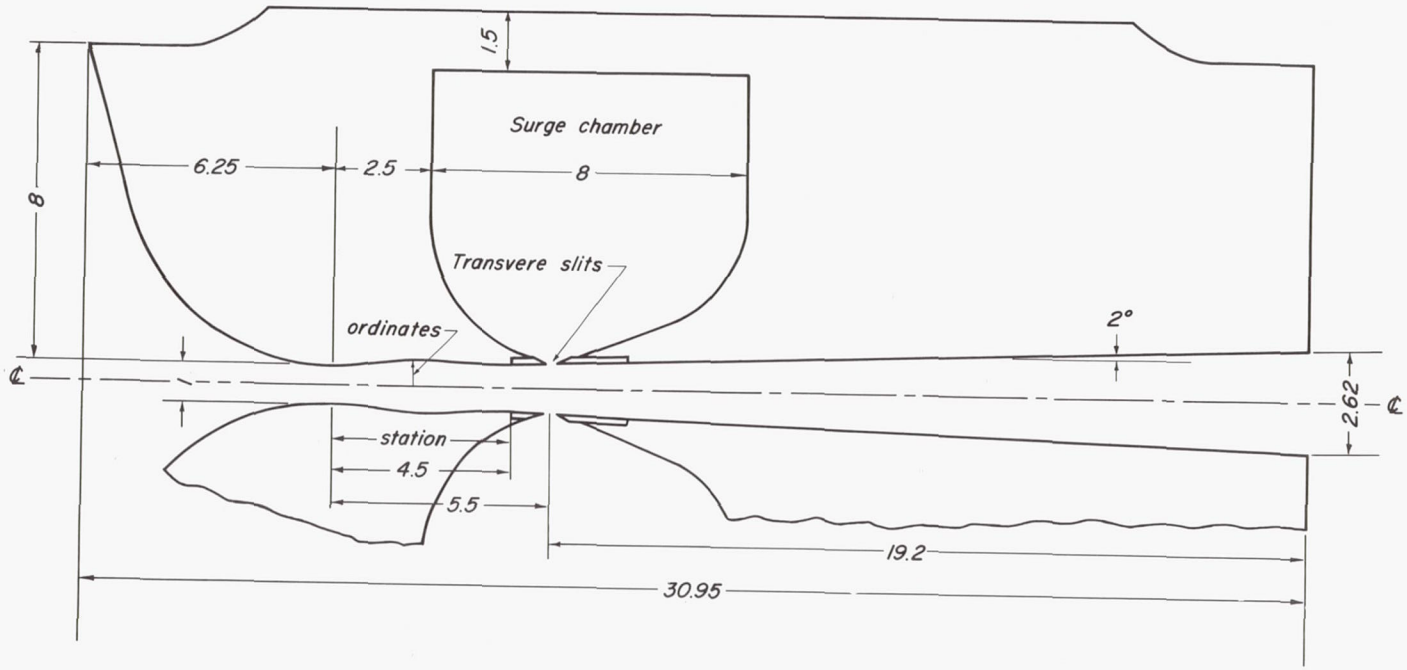


Table of ordinates

Station	Ordinates
0	.500
.2	.510
.4	.530
.6	.555
.8	.580
1.0	.600
1.2	.620
1.4	.635
1.6	.645
1.8	.653
2.0	.660
2.5	.665
3.0	.660
3.25	.652
3.5	.640
3.75	.630
4.0	.620
4.25	.610
4.5	.605

NACA

Figure 1.- Channel shape and nozzle-block design for test section Mach number = 1.64 (all dimensions in inches)

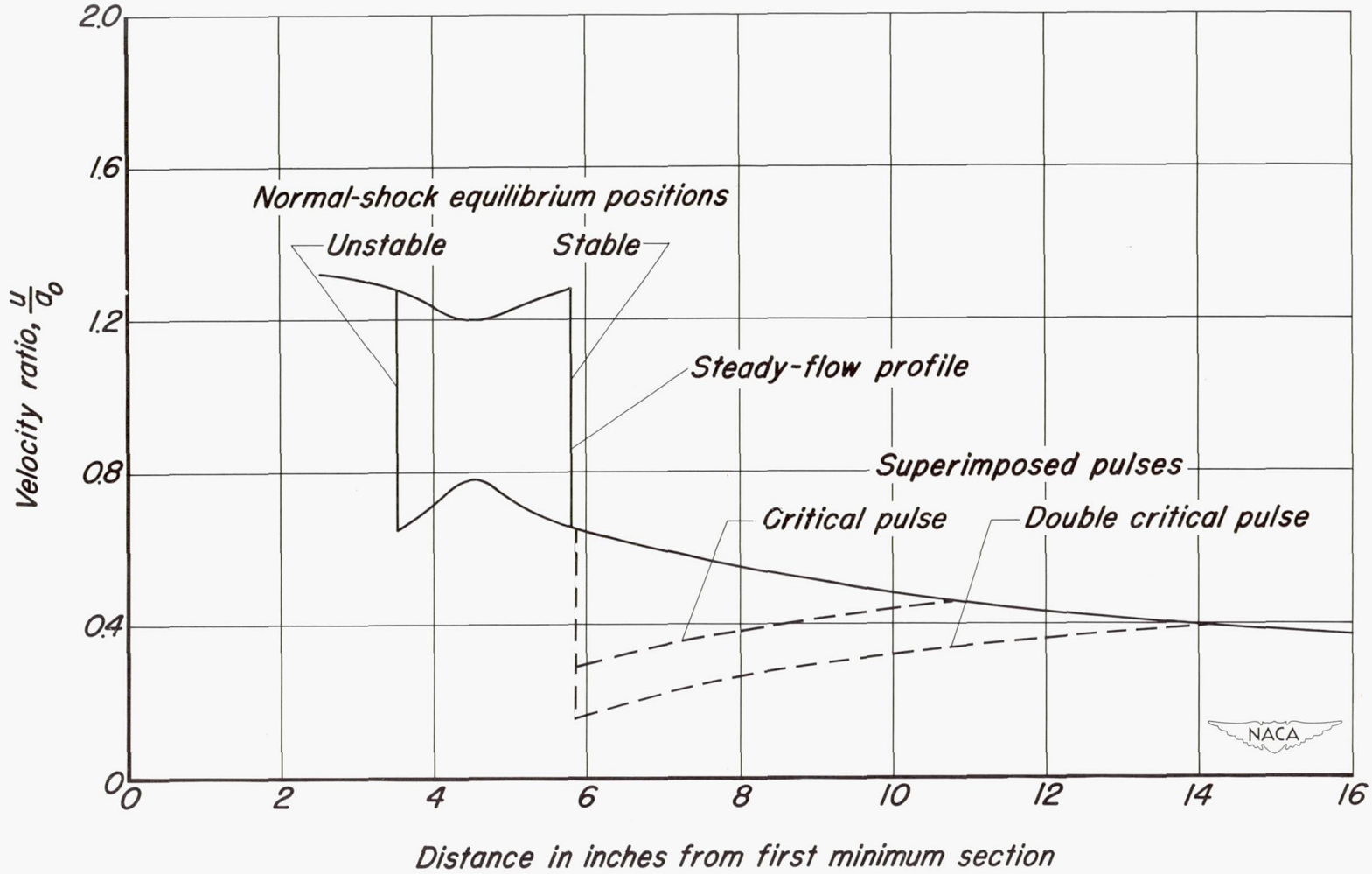


Figure 2.-Velocity profile of channel showing superimposed pulses in position of impending intersection with normal shock in stable equilibrium position.

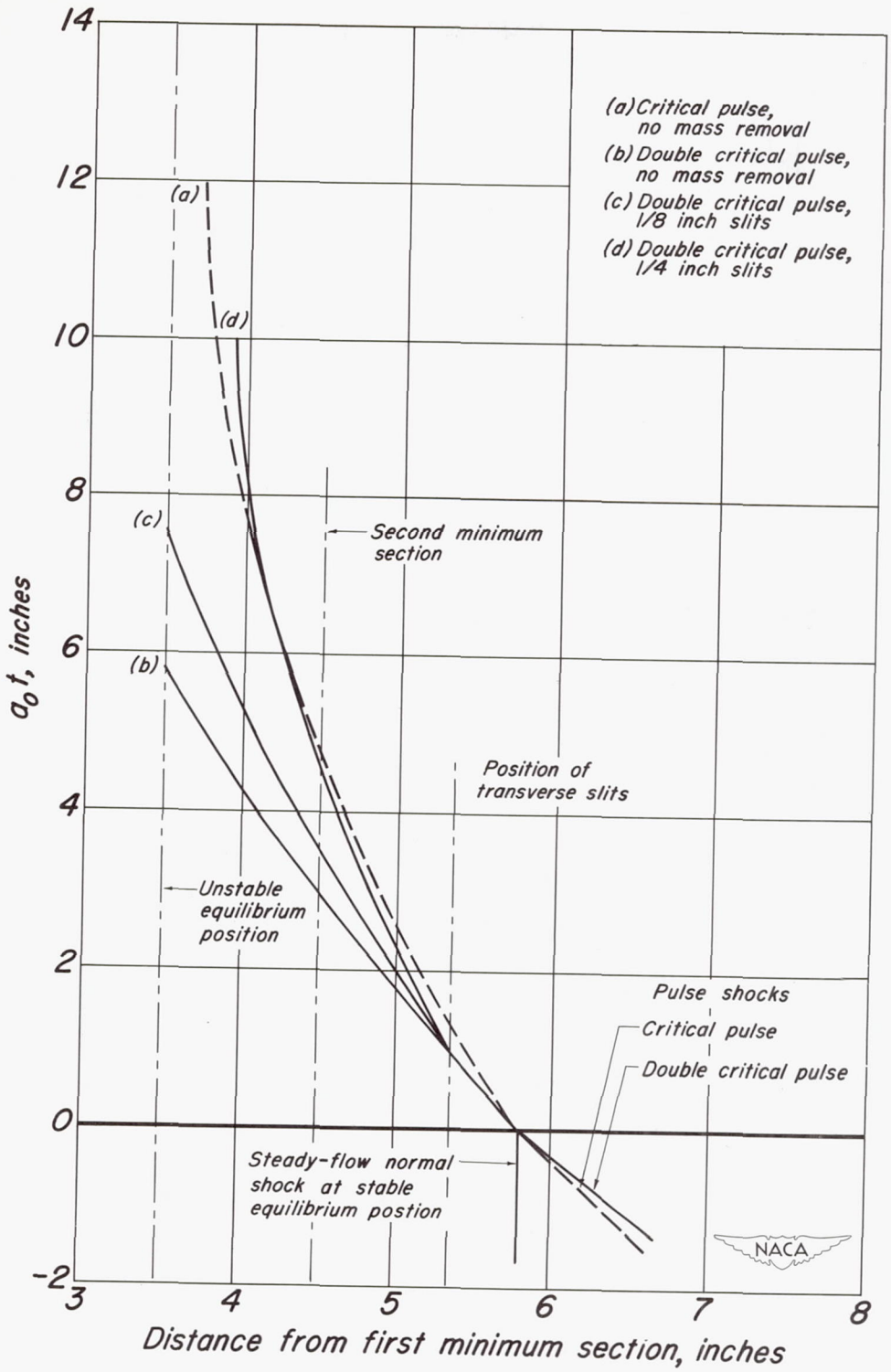
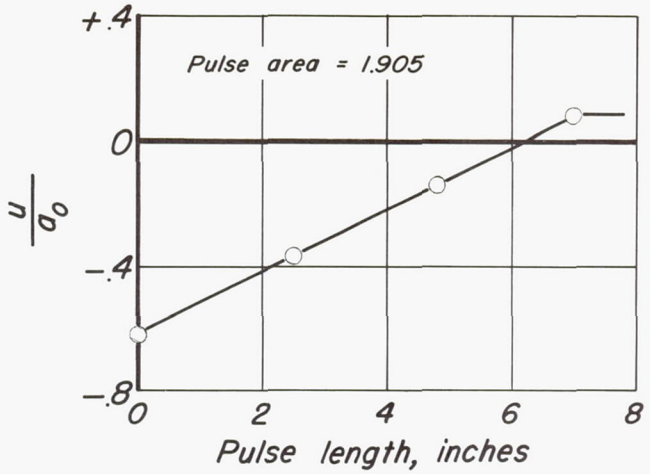
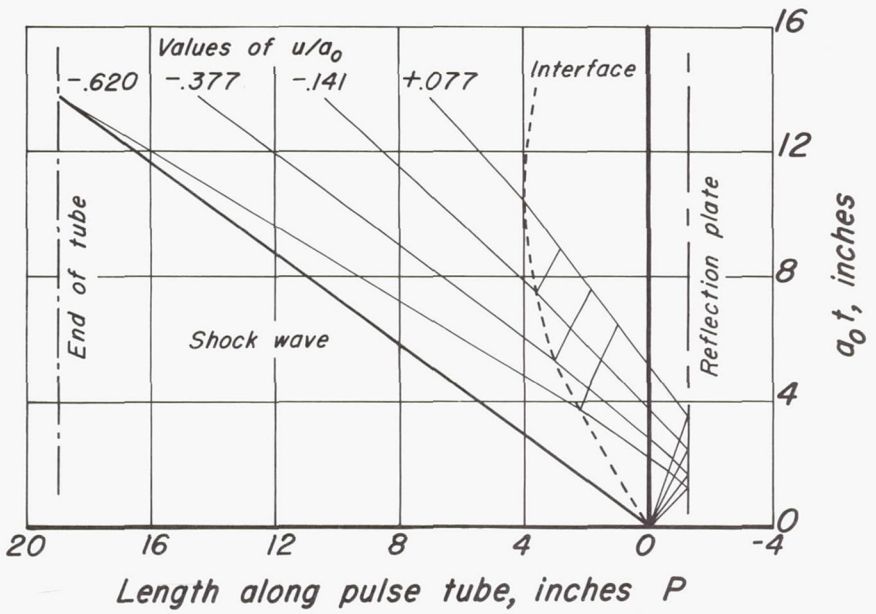


Figure 3.- Interaction of critical and double critical pulse with steady flow normal shock for various amounts of mass removal.



(b) Velocity profile with length dimension corrected by scale factor 0.585 to produce desired pulse area.



(a) Characteristic diagram

NACA

Figure 4.- Analysis to produce pulse with leading-edge velocity discontinuity, $\Delta \frac{u}{a_0}$, of −0.610 and velocity-profile area, ($\frac{u}{a_0}$ vs inches) of 1.905.

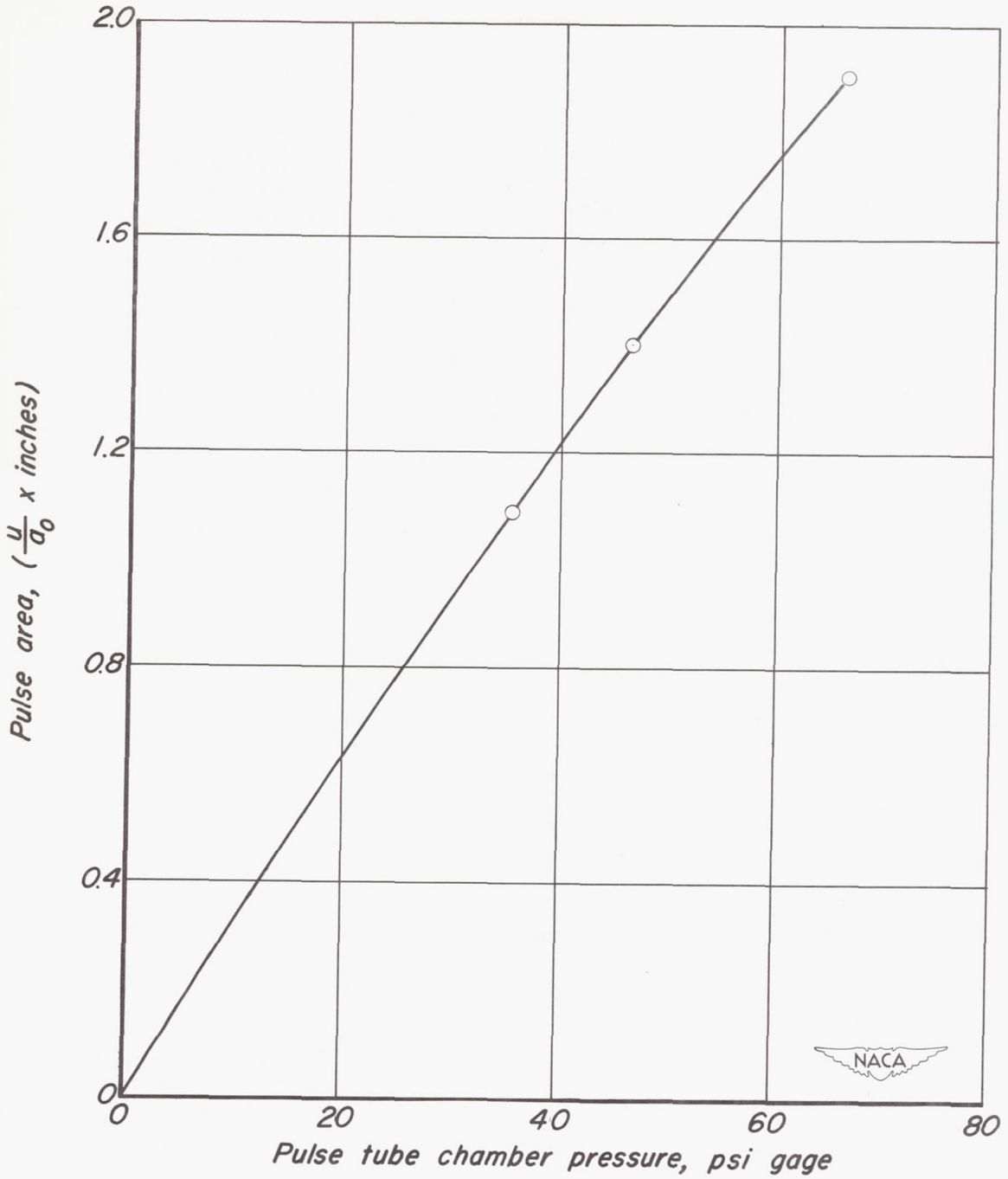


Figure 5.-Relation between pulse tube chamber pressure and velocity-profile area.

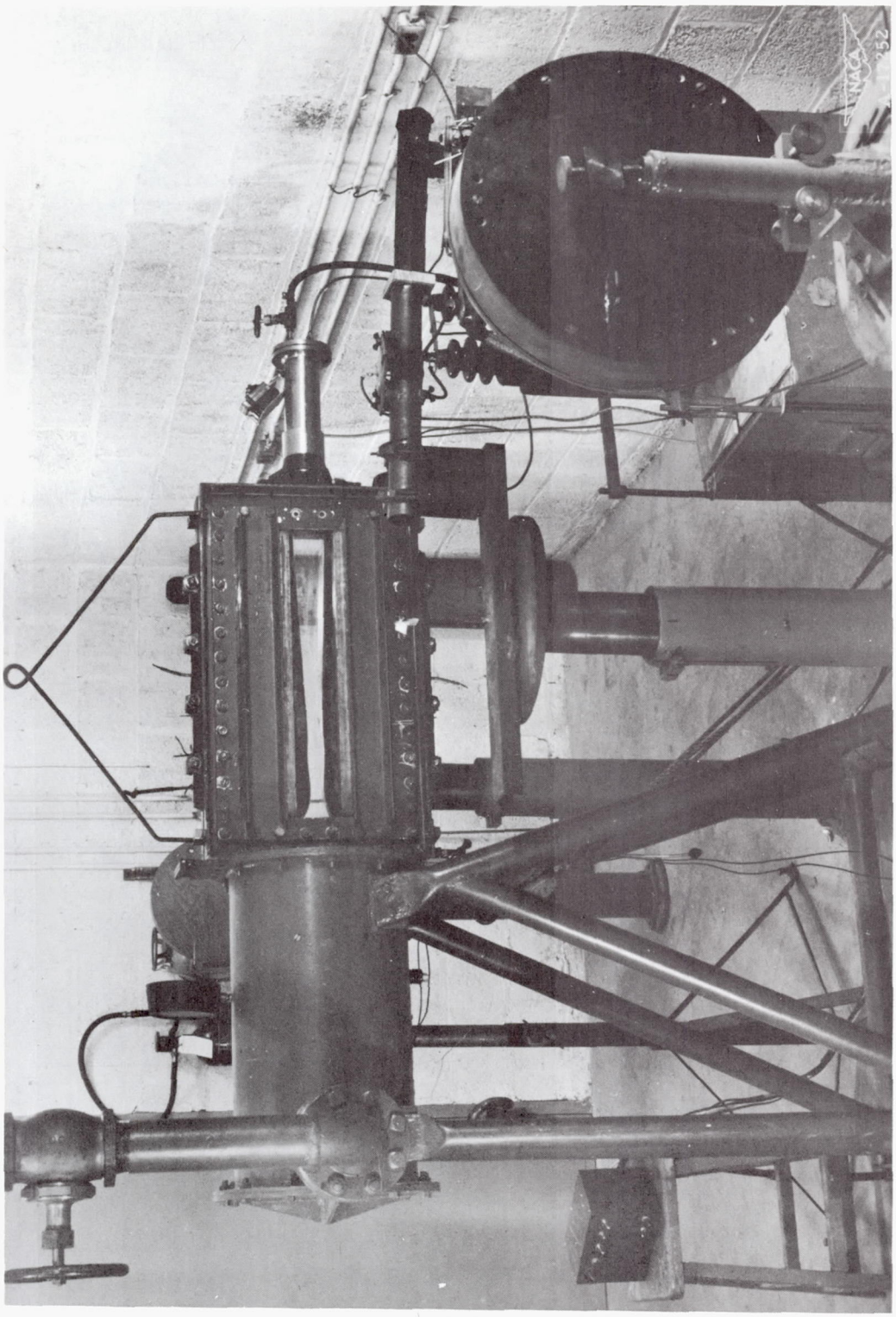


Figure 6.- Experimental apparatus.

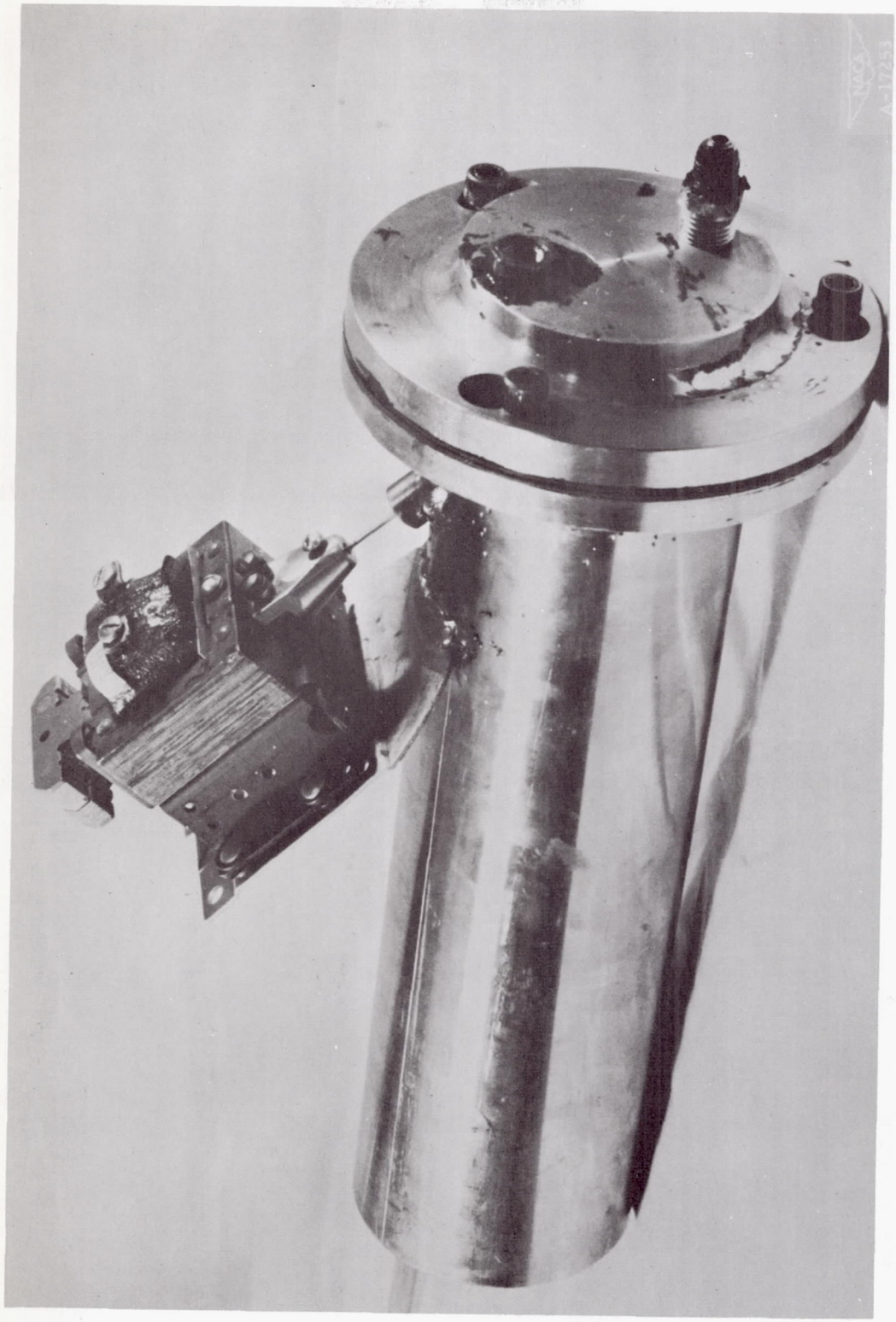


Figure 7.- Pulse tube.

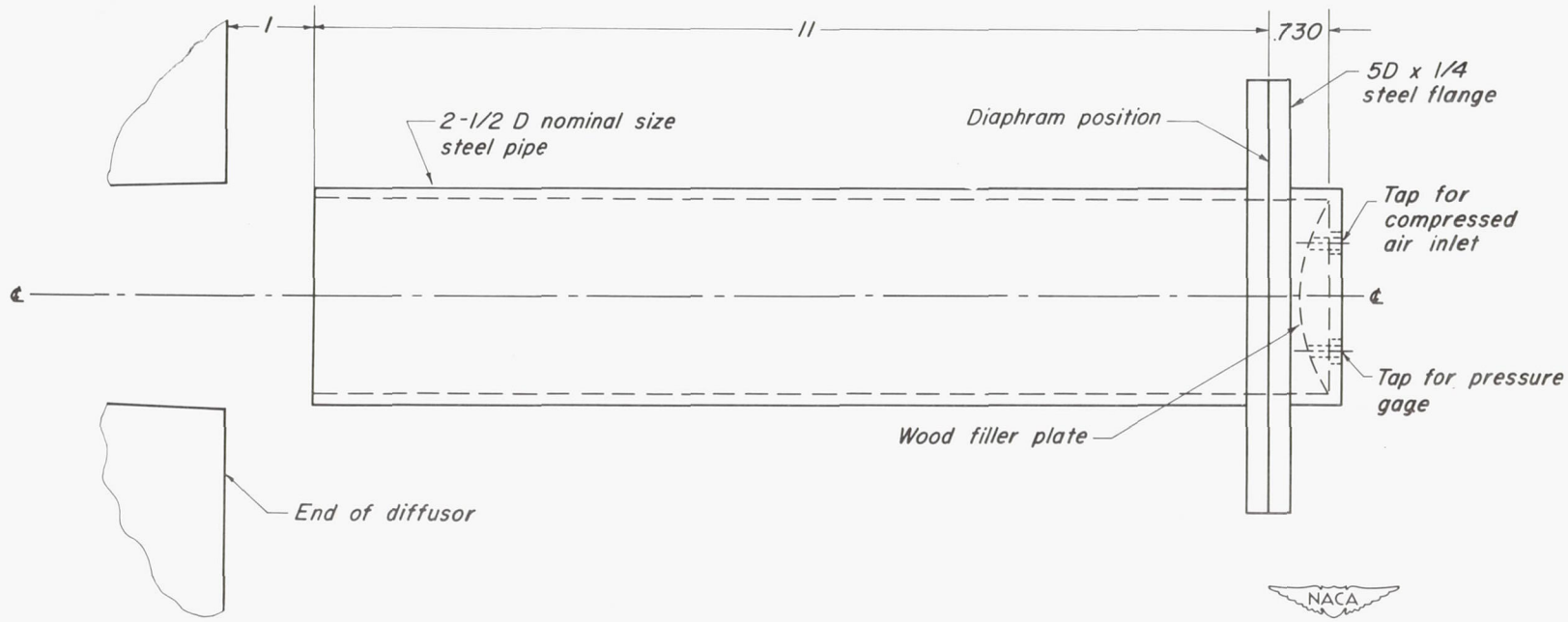
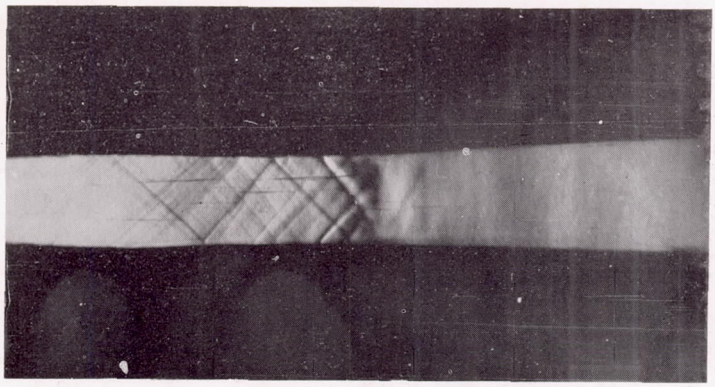
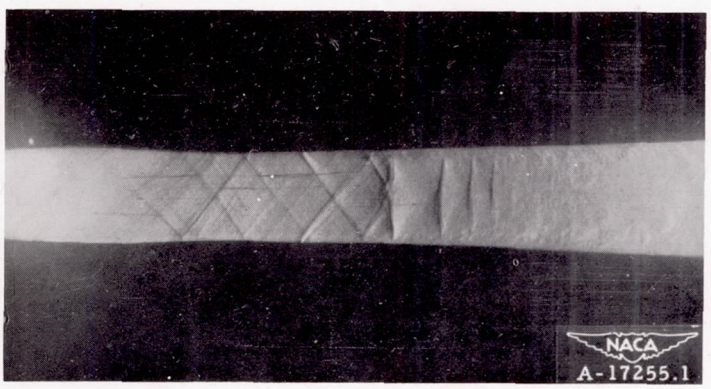


Figure 8.– Design of pulse tube. (all dimensions in inches)

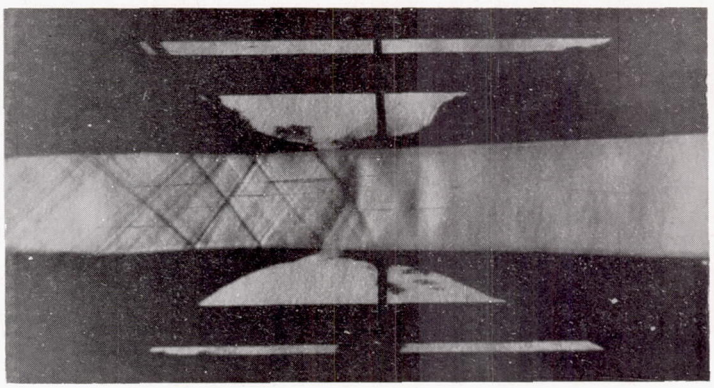


(a) Exposure, 1/25 second.

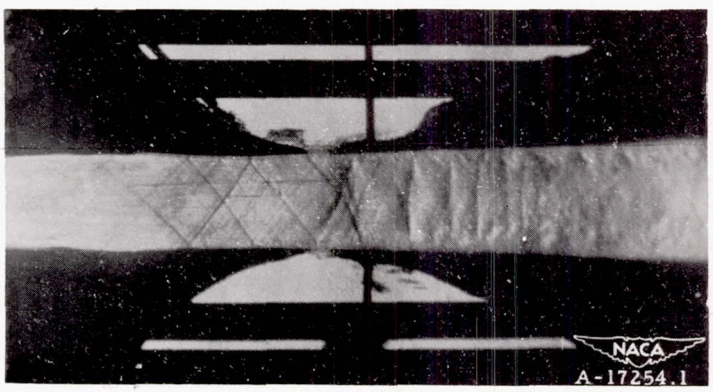


(b) Exposure, 1 microsecond.

Figure 9.- Normal shock in channel under the influence of random disturbances originating downstream; transverse slits closed.



(a) Exposure, 1/25 second.



(b) Exposure, 1 microsecond.

Figure 10.- Normal shock in channel under the influence of random disturbances originating downstream; transverse slits open 1/4 inch.